International Journal of Advanced Multidisciplinary Research
ISSN: 2393-8870
www.ijarm.com
(A Peer Reviewed, Referred, Indexed and Open Access Journal)
DOI: 10.22192/ijamr Volume 9, Issue 8 -2022

Research Article

DOI: http://dx.doi.org/10.22192/ijamr.2022.09.08.005

Impact of climate change on hydrology based on multi-model ensemble of CMIP6 in the Upper Kabul River Basin, Afghanistan.

Shahir Ahmad Taqizada[a], Xuejing Tang[a], Abdullah Ahmadi[b], Hellal Ahmad Taqizada[b], Zhenzhong Hu[a,*].

[a]Tianjin Key Laboratory of Clean Energy and Pollutant Control, School of Energy and Environmental Engineering, Hebei University of Technology, Tianjin 300401, P. R. China
[b] Ministry of Mines and Petroleum (MoMP), Abdulhaq Square, Kabul, Afghanistan
* Corresponding author.
E-mail address: *huzhenzhong@hebut.edu.cn*

Keywords

Climate Change,
LARS-WG6,
SWAT model,
Projection,
Stream Flow.

Abstract

Kabul River Basin (KRB), one of Afghanistan's most important river basins, has been severely impacted by climate change. Yet, the magnitude and intensity of climate change's impact on water resources as a major driver of irrigation and food production are not well understood. Thus, in this study, we used the Soil and Water Assessment Tool (SWAT) hydrological model to assess the implications of climate change for water resources in the upper KRB, Afghanistan. Four general circulation models (CanESM5, MIROC6, MPI-ESM1-2-LR, and NESM3 with SSP2-4.5 and SSP5-8.5) were used for climate data projections of four periods (the 2030s, 2050s, 2070s, and 2090s). LARS-WG was applied to downscale GCM data. The findings revealed that the mean monthly temperature is projected to increase under both SSPs for the 21st century. Annual projected precipitation decreases under the SSP2-4.5, and a decrease for the 2030s and 2050s and an increase for the periods 2070s and 2090s under the SSP5-8.5. For the wet seasons, precipitation is decreasing while it is increasing during the dry seasons. The annual stream flow will decrease from -2.7 to -12.0% under SSP2-4.5 and from -0.3 to -1.8% for the 2030s and 2050s under SSP5-8.5 respectively, whereas it will increase by 5.1% for the 2070s and 4.5% for the 2090s respectively. This study gives crucial information about water resource management and planning in the upper Kabul River Basin in the context of climate change.

1. Introduction

Global warming has become a major concern, posing significant threats to regional and continental water bodies, energy systems, food systems, and biodiversity systems (Hyandye *et al.*, 2018). It is predicted to raise regional and global air temperatures and increase variability in precipitation amounts and regimes (Wang et al., 2020). Assessing the impact of climate change on streamflow is a key part of a proper water resource management plan to reduce its adverse effects (Kurylyk *et al.*, 2014; Golladay *et al.*, 2020). Climate change substantially influences water supplies, not only in precipitation and temperature but also in streamflow (Aawar and Khare, 2020). Besides climate change, human-caused land use/cover change (LUCC) has an impact on hydrologic features such as surface flow, groundwater, and water yield (Wang and Stephenson, 2018). An increase in streamflow directly relates to vegetation and soil infiltration since a large amount of rainfall is converted to runoff, decreasing soil infiltration to recharge groundwater resources (Nyatuame *et al.*, 2020). An assessment of water resource change in the sense of climate change will furnish policymakers with a scientific foundation to develop viable watershed management plans (WMPs) that contribute to various processes, such as ecological systems and agricultural sectors.

General circulation models (GCMs) are the primary mathematical models used to forecast climate impacts. Various modeling groups examine the effects of the previous era, present, and upcoming global warming on a global or synoptic scale as part of the combined model intercomparison project (CMIP). Moreover, its results are being used to analyze the influence of climate change on water resources by utilizing hydrological models (Eyring *et al.*, 2016; Alamdari *et al.*, 2017). In recent years, there has been an increasing number of GCM models available (Eyring *et al.*, 2016). The Intergovernmental Panel on Climate Change (IPCC) is currently working on its sixth assessment report (IPCC), referring to outcomes from the sixth phase (CMIP6) (The CMIP6 landscape, 2019). After almost a decade of model development relative to CMIP5, three aspects of progress in CMIP6 have been noted in comparison with CMIP5, including the number of modeling centers registered for simulation, which has risen by more than one-third. Meanwhile, the CMIP6 uses scenarios focused on socio-economic trends: the shared socio-economic pathways (SSP1-SSP8) through shared policy assumptions combined with RCPs. As a result, multiple business-as-usual scenarios will be feasible in CMIP6 for climate change projection. And also, finer resolution and enhanced physical processes were used in the design (The CMIP6 landscape, 2019). GCMs can be applied to hydrologic processes by rescaling spatial data from coarse to catchment scales (Yu *et al.*, 2020).

High-resolution climate data improves the quality of hydrological projections, allowing for a more accurate projection of water resources in a watershed. The direct application of general circulation models (GCM) at a watershed level to study the hydrological responses to climate change without high-resolution climatic input data is limited due to their coarse resolution (Willems. P and Vrac. M, 2011; Skoulikaris *et al.*, 2020). Therefore, downscaling and bias correction of climate model simulation is strongly advised before using it for hydrological effect assessment. Otherwise, there will be a considerable disparity between the GCM's performance and historical observations (Teutschbein and Seibert, 2012; Ramirez-Villegas *et al.*, 2013). Hydrological models are generally used for the combination of climate change and hydrological processes. The SWAT model can simulate hydrological procedures and incorporate them into the climate change impact simulations (Ficklin *et al.*, 2010), which is commonly used across the entire globe. (Abbaspour *et al.*, 2018).

Afghanistan is a semi-arid country with a high level of precipitation variability and inconsistency. The surface water of Afghanistan is separated into five major river basins based on morphology and hydrology systems: the Amu-

Darya River Basin, Kabul, Helmand, Harirud-Murghab, and Northern (Nasimi *et al.*, 2020). The Kabul River Basin (KRB) is among the most crucial river basins in the country, and it is a shared river basin with Afghanistan and Pakistan. KRB serves as a water source for over 20 million people and is primarily used by both countries for hydropower generation and irrigation (Wi *et al.*, 2015). As a result, determining how climate change will affect water resources in this catchment is crucial for proactive water management. Over the last few decades, several dams have been constructed or planned to be built in the KRB. Streamflow changes may affect the efficiency of sediment trapping, hydropower generation, and storage facilities in reservoirs. Accordingly, the investigation of climate changeimpacts on streamflow is essential for appropriate design and dam operation (Nafees *et al.*, 2016). The Kabul River's flow mostly comes from snowmelt in the mountains in winter and early spring precipitation. However, the precipitation that falls on the mature snowpack in the mountains during late winter and early spring can contribute to higher water levels in the streams (Lashkaripour and Hussaini, 2008).

The effects of climate change on the KRB runoff have been assessed in several studies (e.g., Ghulami, 2017; Alokozay and J, 2020; Hashmi *et al.*, 2020; Bromand, 2015). Ghulami (2017) analyzed climate change impacts for three periods (the 2020s, 2050s, and 2080s) using eight GCM models in CMIP5 under RCP4.5 and RCP8.5, and the results showed a likely increase in runoff in the KRB, mainly due to the temperature increase, which causes more snow and ice melting in the catchment. Alokozay and J (2020) investigated the runoff responses to climate change for the period (2046-2064) using four GCM models and three climate scenarios (A2, A1b, and B1). They found an increase in runoff in January, February, March, and April months between (35% to 45%), and an expectation of a decrease in June, July, August, and September months between (40% to 50%). Bromand (2015) used three climate scenarios (A2, A1B, and B1) based on four GCM models and found that streamflow in the study area would decrease by approximately 24 percent during the period (2046–2064). Hashmi *et al.* (2020) conducted another investigation of streamflow in the face of climate change in the KRB based on four GCMs and two emission scenarios (RCP 4.5 and RCP 8.5) for two time periods (2011-2030 and 2031-2050) in which river discharge is anticipated to increase in the study region.

In the KRB, there are presently very few studies on how streamflow changes in response to climate change. Notably within the upper stream inside Afghan territory. The upstream of KRB is important not only for local purposes but also for maintaining the water supply, flood control, and ecological services for the downstream. Since CMIP6, the latest state of GCMs has introduced improvements in various aspects (Gusain *et al.*, 2020). The study's authors expect that this advancement in the new state of GCMs will yield more reasonable and reliable results in the upper KRB. This is the first study using CMIP6 models to investigate future climate change (precipitation and temperature) and its influence on water resources in the upper subbasin of KRB, which has not been done before. This was attained by applying the hydrological model Soil and Water Assessment Tool (SWAT) driven by four GCM projection models under two Shared Socioeconomic Pathways scenarios (SSP2-4.5 and SSP5-8.5) generated by the Long Ashton Research Station Weather Generator (LARS-WG). Therefore, the findings of this study could be utilized by water managers to develop a comprehensive plan for managing water resources in the KRB.

2. Materials and Methods

2.1. Study area

The current study focuses on the upper subbasin of KRB (Figure 1). The total basin of the study area is 850 km^2, *with the highest elevation of 4485 and a minimum elevation of 1740 MASL*. Kabul, the largest city and capital of Afghanistan, has a population of 4.2 million and a semi-arid and continental climate.The KRB is situated in eastern Afghanistan between longitude 67º 40' to 71º 42' E, and latitude 33º 33' to 36º 02' N. It originates from the Paghman mountain range (Sanglakh region), 72.42 km west of Kabul City, which is part of Afghanistan's Hindu-Kush Mountains. After passing through Kabul and Jalalabad, the Khyber Pass into Pakistan, and Peshawar joins the Indus River northwest of Islamabad (Lashkaripour and Hussaini, 2008; Rasouli et al., 2015; Zaryab et al., 2017). A total of 67,370 km^2 of the drainage area is associated with the Kabul River, which has a length of 700 km and flows for 560 km inside Afghanistan (Wi et al., 2015). With mean annual streamflow of 24 billion cubic meters, KRB represents about 26 percent of Afghanistan's total water resources. It accounts for 12% of Afghanistan's total land (Sidiqi et al., 2018).

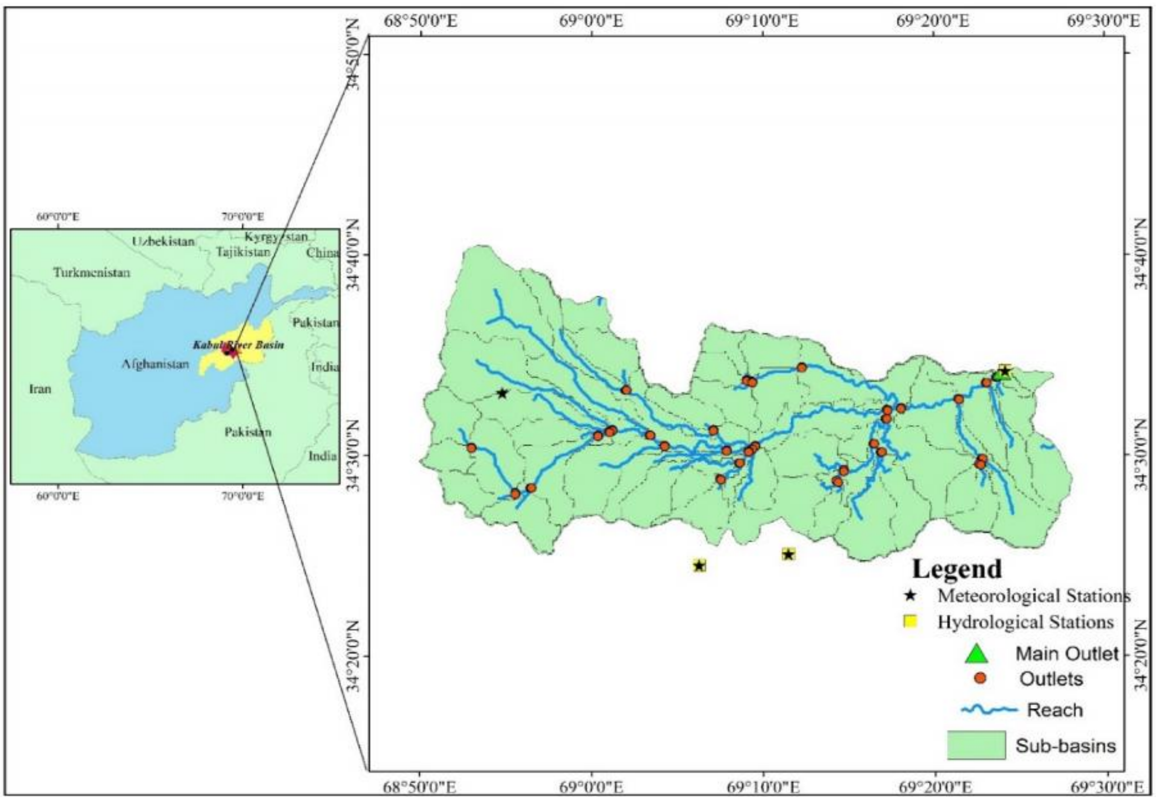

Figure 1. Study area.

2.2. Datasets

We obtained daily recorded meteorological data, including maximum and minimum (Tmax & Tmin) air temperatures, daily precipitation, and relative humidity data, at four metrological stations located in and near the study area from the Ministry of Energy and Water of Afghanistan (MoWE) for the period (2004-2020).

Daily projected future climate data (Tmax, Tmin, and precipitation) derived from the GCMs' sixth Assessment Report (AR6). Four climate models (CANESM5, MPI-ESM1-2LR, NESM3, MIROC6) have been selected from the CMIP6, for the historical period 1929-2014 and the future period 2022-2099, under two Shared Socioeconomic Pathways (SSP5-8.5 and SSP2-4.5) (https://esgfnode.llnl.gov/search/cmip6/). SSP5-8.5 is subjected to the highest-radiation emission scenario with 8.5 Wm^{-2} of radiative forcing at the end of the century. SSP2-4.5, with 4.5 Wm^{-2} of radiative forcing till 2100, embodies a moderate emissions scenario, which results in medium to high social vulnerability and the difficulty of mitigation (O'Neill *et al.*, 2016). Among the scenarios, the SSP5-8.5 describes the effects of unconventional development as the worst possible future scenario. As a result, it is used to prepare plans to mitigate and adapt to climate change in the worst-case scenario (Touma *et al.*, 2015; Ma *et al.*, 2021). The SSP2-4.5, which has raised broad concerns in most countries attempting to achieve sustainable development, must also be focused on (Riahi *et al.*, 2017). Therefore, we used the SSP2-4.5 and SSP5-8.5 scenarios to study the effect of climate change on water resources in the upper subbasin of KRB.

The Digital Elevation Model (DEM) with a 90 m spatial resolution was obtained from (https://earthexplorer.usgs.gov/) and used to create the watershed delineation and topographic characterization in Arc SWAT 2012. The DEM map is generated using Arc GIS 10.7 (Figure 2a).

The soil dataset was obtained from the Food and Agriculture Organization (FAO) (https://www.fao.org). And the study area soil map is extracted by using Arc GIS 10.7 (Figure 2b). The type of soil, coupled with the physical and chemical characteristics of the soil, such as hydraulic conductivity, water content, bulk density, and soil material percentage (clay, sand, silt), has an important impact on streamflow (Galata *et al.*, 2020).

The supervised land cover classification for the SWAT model for 2019 has been created by Google Earth Engine (GEE), using Landsat 8 OLI (Figure 2c). The Random Forest Classifier (RFC) method is used for the classification (Phan *et al.*, 2020). A cloud mask is used to prevent cloud contaminants (Mateo-García *et al.*, 2018). The accuracy assessment showed 80.1% for the study area LULC. Monthly river discharge data is provided by the MoWE for four hydrological stations from 2004 to 2018 for SWAT model inlet, calibration, and validation periods.

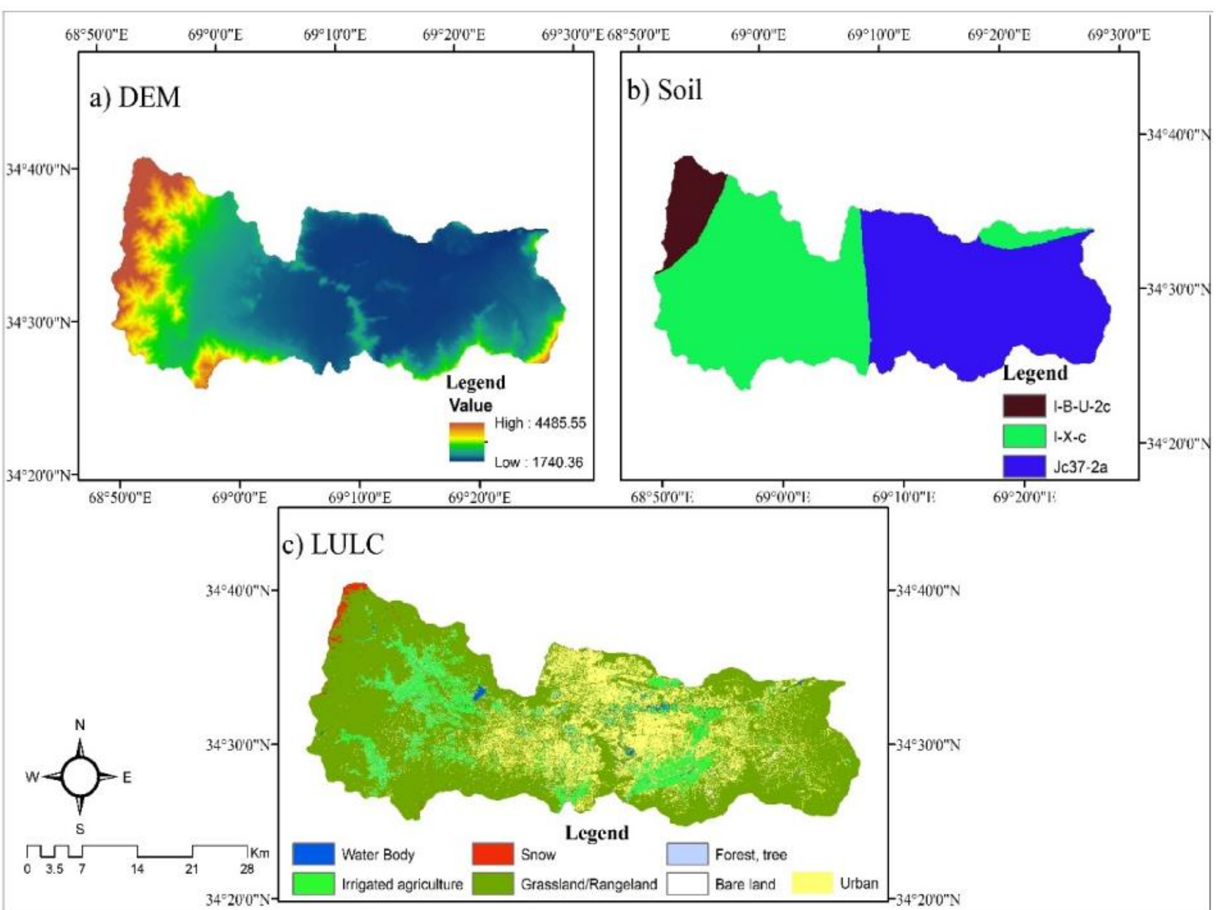

Figure 2. a) Elevation map, b) Soil map, and c) LULC map of upper Kabul River Basin (KRB).

2.3. General methodology

The research methodology used in this study illustrates in Figure3. The Soil and Water Assessment Tool (SWAT), a comprehensive hydrological model, is employed to simulate streamflow. This model is widely used to assess and predict the impact of various management scenarios on water resources (Arnold *et al.*, 1998). The Sufi2 algorithm provided by SWAT-CUP was used to calibrate and validate the simulated streamflow (Khalid *et al.*, 2016). In the next section, a statistical downscaling model, LARS-WG, was used to produce future climate data derived from GCM models to assess climate change. The output data for maximum and minimum temperatures and daily precipitation are compared to the baseline period under the SSP2-4.5 and SSP5-8.5 scenarios. In the third section, the calibrated SWAT model was then employed in SWAT projection modeling, driven by stochastically generated future climatic scenarios under SSP2-4.5 and SSP5-8.5. In a comparison between the baseline and the future streamflow simulations, the effect of climate change on streamflow was finally assessed during four future periods: the 2030s (2022-2039), the 2050s (2040-2059), the 2070s (2060-2079), and the 2090s (2080-2099).

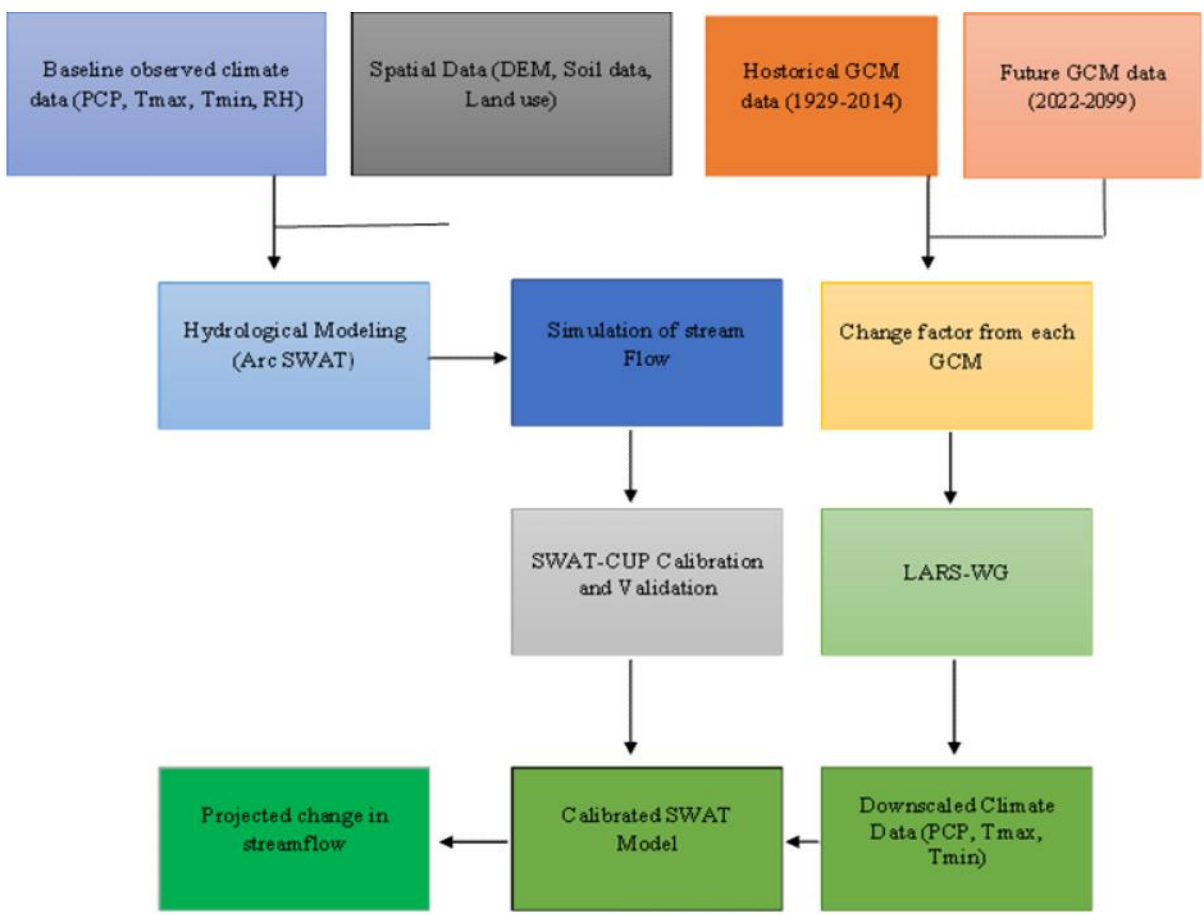

Figure 3. Research methodology framework.

2.4. Stochastic weather generation

The Global Climate Model (GCM) outputs are produced at a coarse spatial resolution. It is difficult to accurately correlate the direct usage of GCM outputs with regional climate change implications (Zhang *et al.*, 2019). Consequently, a downscaling technique is required to rectify the disparity between the GCM outputs and the inputs to the hydrological models (King *et al.*, 2012).

Various statistical downscaling methods are available to develop climate projection data based on the stations (Khoi, 2019a). As part of this study, the Long Ashton Research Station Weather Generator (LARS-WG) is used to generate temperature and precipitation data for future periods and a hydrological model based on different climate scenarios. The stochastic weather generator developed by Semenov and Stratonovich is based on the series method (Khoi, 2019a). It can generate a better result since it is capable of creating synthetic daily rainfall series that are substantially similar to the measured data. The LARS-WG model uses daily time series of temperatures (Tmin and Tmax), precipitation, and solar radiation at a single station. LARS-WG generates daily precipitation data using a semi-empirical distribution model. On the other hand, temperature series are constructed using a finite Fourier series, which is different from the precipitation solution method (Baghanam *et al.*, 2020). This model has been tested in various climates and provides reliable weather statistics, including extreme weather occurrences (Khoi, 2019b).

We calculated the monthly mean temperatures (Tmax and Tmin), precipitation, wet and dry periods, and daily mean temperature standard deviations for each GCM throughout the historical and future periods. Then these change factors of climate data are applied to each of the four GCM models to generate the future climate for periods (the 2030s, 2050s, 2070s, and 2090s) considering the baseline period (2004-2020). They have been used to perturb LARS-WG site characteristics to produce future daily climate data for each GCM.

2.5. SWAT model

This study uses the Soil and Water Assessment Tool (SWAT) (version 2012) to simulate the response of streamflow to climate change in the upper subbasin of KRB. In SWAT, a semi-distributed, physically based, and long-term simulation model, water, agricultural chemical yields, and sediment in large basins are simulated by taking into account various soil types, land uses, and management conditions (Arnold *et al.*, 1998). For assessing and simulating the response of hydrology to climate change, the SWAT model has been validated and proven reliable in many countries (Shrestha *et al.*, 2013; Gassman *et al.*, 2014; Tan *et al.*, 2019; Tan *et al.*, 2020). The SWAT model divides the basin into several subbasins depending on the river systems and topography of the basin. And each subbasin is divided into hydrologic response units (HRUs) with different soil types, slope classes, and land-use characteristics. The flow is computed first at HRUs and then added to the relevant subbasin and finally added to the basin's outlet (Neitsch *et al.*, 2011). SWAT uses the water balance equation to simulate the hydrologic cycle, as given in Equation (1), which includes processes such as precipitation, evapotranspiration, surface runoff, infiltration, lateral flow, percolation, and groundwater flow (Neitsch *et al.*, 2011).

$$SWt = SW0 + \sum_{t=1}^{t}(P - Qsurf - ET - Wap - Qgw) \quad (1)$$

SW0 and SWt are the initial and final soil water content (mm), t is the time (days), Rday is daily precipitation(mm), Qsurf is the amount of surface runoff on a day, ET is the amount of evapotranspiration on a day, Wap is the amount of water entering the vadose zone from the soil profile on a day (mm), and Qgw is the amount of return flow (or base flow) on a day i (mm).

SWAT uses the modified Soil Conservation Service (SCS) curve number (CN) method to calculate surface runoff from daily rainfall (SCS, 1972). The SCS–CN equation is an efficient and robust method for predicting runoff from daily precipitation data based on Equation (2) (Arnold *et al.*, 1998)

$$Q = \frac{(R - 0.2S)^2}{(R - 0.8S)^2} \quad (2)$$

where Q = surface runoff in (mm), and R = depth of daily rainfall (mm). S = retention parameter, which is defined in Equation (3).

$$S = 254\left(\frac{100}{CN} - 1\right) \qquad (3)$$

CN = curve number (100 ≥ CN ≥ 0, CN = 100 indicate zero potential retention, and CN = 0 indicate an infinite catchment with S = ∞.)

2.6. Model setup, Sensitivity analysis, Calibration, and Validation

The SWAT model input data for the period 2006 to 2020 consists of digital elevation models (DEM), land use maps, soil maps, and several metrological datasets, such as precipitation, Tmin, Tmax, and relative humidity. As defined by the FAO, the soils of the study area are classified into three categories (I-B-U2-c, I-X-c, and Jc37-2a). And land-use was classified into seven different classes. The SWAT model divided the research area into 63 sub-basins and 172 HRUs. For the purpose of calibrating and validating models, we used the Tangi Gharo Hydrological Station, the outlet of the study area.

The precision of SWAT simulations is dependent to a great extent on the calibration and validation processes (Zhang *et al.*, 2019). For SWAT model calibration, validation, and sensitivity analysis, we used the SWAT Calibration and Uncertainty Program (Abbaspour *et al.*, 2007) (SWAT-CUP). Several sensitivity analyses were performed along with calibration in order to identify the most influential parameters. For calibration and uncertainty analysis, the SUFI2 algorithm was used, which is commonly used to calibrate SWAT models (Sao *et al.*, 2020). The SWAT model was performed daily. At Tangi Gharo Hydrological Station, the calibration and validation of the model were carried out monthly, as there was no reliable daily streamflow data. Calibration and validation were performed using monthly streamflow records from 2006 to 2014 and 2015 to 2018. The warm-up period was from 2004 to 2005.

Evaluation of model performance was based on Nash-Sutcliffe Efficiency (NSE), coefficient of determination (R2), root mean square error to standard deviation of observed data (RSR), and percentage bias (PBIAS), which are explained in Equations. (4, 5, 6, and 7). In accordance with Moriasi's recommendations, there are four performance ratings for the model (Excellent, Good, Satisfactory, and Unsatisfactory) (Moriasi *et al.*, 2007) (Table 1).

$$NSE = 1 - \frac{\sum_{i=1}^{n}(Q_{Oi} - Q_{si})^2}{\sum_{i=1}^{n}\left(Q_{Oi} - Q_{avg}\right)^2} \qquad (4)$$

$$PBAIS = \frac{\sum_{i=1}^{n}(Q_{Oi} - Q_{si})}{\sum_{i=1}^{\infty}(Q_{Oi})} * 100 \qquad (5)$$

$$R^2 = \frac{\left[\sum_{i=1}^{n}\left(Q_{Oi} - Q_{avg}\right)\left(Q_{Si} - Q'_{avg}\right)\right]^2}{\sum_{i=1}^{n}\left(Q_{Oi} - Q_{avg}\right)^2 \sum_{i=1}^{n}\left(Q_{Si} - Q'_{avg}\right)^2} \qquad (6)$$

$$RSR = \frac{\sqrt{\sum_{i=1}^{n}(Q_{Oi} - Q_{si})^2}}{\sqrt{\sum_{i=1}^{n}\left(Q_{Oi} - Q_{avg}\right)^2}} \qquad (7)$$

where Observed and simulated values are Qoi and Qsi at the month i, observed values are Qavg, simulated values are Q' avg, and n is the number of data values.

Table 1. Monthly statistics model performance rating.

P. RATING	NSE	R2	PBIAS	RSR
Excellent	0.75<NSE≤ 1.00	0.75＜R2 ≤ 1	PBIAS<± 10	0 <RSR≤ 0.5
Adequate	0.65 <NSE≤ 0.75	0.65＜R2 ≤ 0.75	±10≤ PBIAS< ± 15	0.5 < RSR ≤ 0.6
Satisfactory	0.50 <NSE≤ 0.65	0.5＜R2 ≤ 0.65	±15 ≤ PBIAS< ±25	0.6 < RSR ≤ 0.7
Unsatisfactory	NSE≤ 0.50	R2 ≤ 0.5	PBIAS> ±25	RSR >0.7

3. Results and Discussion

3.1. Precipitation and temperature bias correction

A comparison of the bias-corrected and uncorrected ensemble of GCMs with observed precipitation data for the period 2004-2020 is shown in Figure4. The observed data and the uncorrected GCMs had a significant difference. The results show that the average monthly precipitation before downscaling in January, February, March, July, and August is underestimated, while the remaining months are overestimated compared to the observed precipitation under SSP5-8.5. For the SSP2-4.5, the average monthly precipitation for September, October, November, and December are overestimated, and the precipitation for the remaining months is underestimated. The results show that both SSPs (SSP2-4.5 and SSP5-8.5) mean monthly precipitation and observed follow similar patterns after being downscaled, which demonstrates the accuracy of LARS-WG in generating climate normals. The results after downscaling show that the average monthly rainfall in January, February, July, August, October, and December is overestimated, while the average monthly precipitation for the remaining months is underestimated at the observed station under both SSPs scenarios. The uncorrected SSPs of maximum temperatures from June to September are overestimated, while the remaining months are underestimated. Similarly, the minimum uncorrected temperature from May to October is overestimated, and it is underestimated for the other months. After downscaling, the maximum and minimum temperatures for the baseline under both SSPs are overestimated compared to ground measured data (Figure 5).

In order to validate the performance of the GCM simulations on precipitation and temperature, some statistical tests (the R^2, RMSD, NSE, and MBE) were performed (Table 2). The values were determined by comparing the simulated climate data based on the two SSP scenarios with the actual values recorded at the station. According to the results, it is feasible to assess the impact of climate change in the study area using the output of GCM simulations.

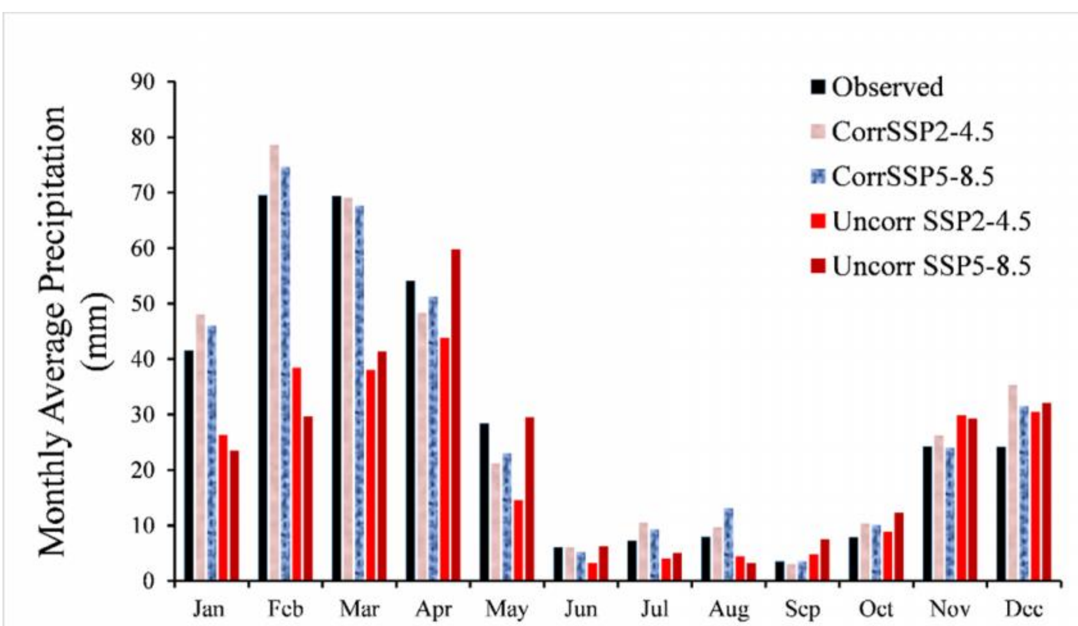

Figure 4. downscaled precipitation.

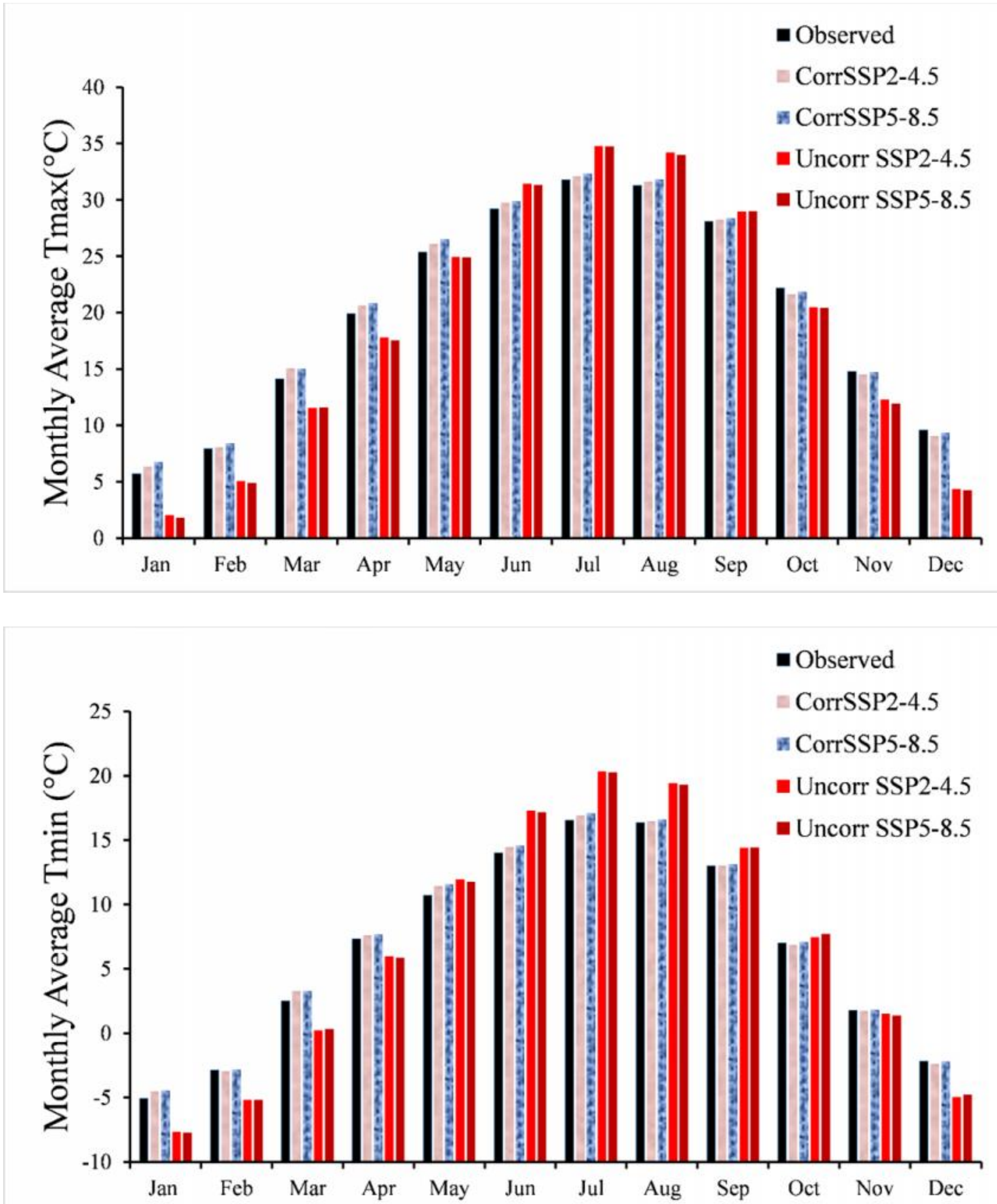

Figure 5. downscaled maximum and minimum temperature.

Table 2. Descriptive statistics and uncorrected/corrected precipitation and temperature by the downscaling model (LARS-WG6).

Climate variables		Scenarios	Statistical Tests			
			R^2	NSE	RMSD	MBE
Precipitation	Uncorrected	SSP2-4.5	0.624	0.104	15.55	5.367
		SSP-58.5	0.798	0.018	14.69	8.083
	Corrected	SSP2-4.5	0.956	0.946	5.457	1.858
		SSP-58.5	0.976	0.974	3.828	1.25
Maximum Temperature	Uncorrected	SSP2-4.5	0.993	0.941	2.776	1.008
		SSP-58.5	0.994	0.938	2.85	1.125
	Corrected	SSP2-4.5	0.997	0.996	0.545	0.258
		SSP-58.5	0.998	0.994	0.668	0.492
Minimum Temperature	Uncorrected	SSP2-4.5	0.993	0.94	2.339	-0.13
		SSP-58.5	0.993	0.94	2.28	-0.12
	Corrected	SSP2-4.5	0.998	0.997	0.406	0.233
		SSP-58.5	0.998	0.996	0.49	0.367

3.2. Temperature projection

The maximum and minimum mean monthly projected temperatures in the upper KRB are anticipated to increase in the twenty-first century relative to the baseline. The ensemble-mean monthly projected maximum temperature increases by 2.4°C under SSP2-4.5 and 3.6°C under SSP5-8.5 in the 2030s. By mid-century, the temperature increases by 2.9°C for SSP2-4.5 and 4.5°C for SSP5-8.5. In the 2070s, temperature increases by 3.1°C under SSP2-4.5 and 4.8°C under SSP5-8.5; and 3.2°C for SSP2-4.5 and 5.0°C relate to SSP5-8.5 in the 2090s (Figure6). Similarly, under SSP2-4.5, the ensemble-mean monthly projected minimum temperature is projected to rise by 2.0°C by 2030s and by 2.9°C under SSP5-8.5. In the midcentury period, 2.5°C and 3.5°C of warming are expected in the SSP2-4.5 and SSP5-8.5 scenarios, respectively. From the 2070s to the end of the century, temperature increases by 2.7°C to 2.8°C under SSP2-4.5 and 3.8° to 4.0°C under SSP5-8.5 (Figure7). For all the months, the long-term mean monthly temperature (maximum and minimum) increased relative to the baseline under both SSPs. The most significant increase in mean monthly Tmax is by 4.0°C in the SSP2-4.5 and 5.9°C in the SSP5-8.5 scenarios for the March months in the 2090s. Similarly, the mean monthly minimum temperature increases under both emission scenarios for all months, where the largest increase is 3.2°C and 4.4°C in the 2090s for the February months. Overall, the rise in temperatures in winter and spring is more significant than in other seasons. Increases in maximum and minimum temperatures probably raise the percentage of evapotranspiration and snow melting and increase the risk of drought during the dry season. Furthermore, an increase in temperature will probably have an impact on the area's water demand. A proper water management strategy is required in order to respond to such an impact of climate change.

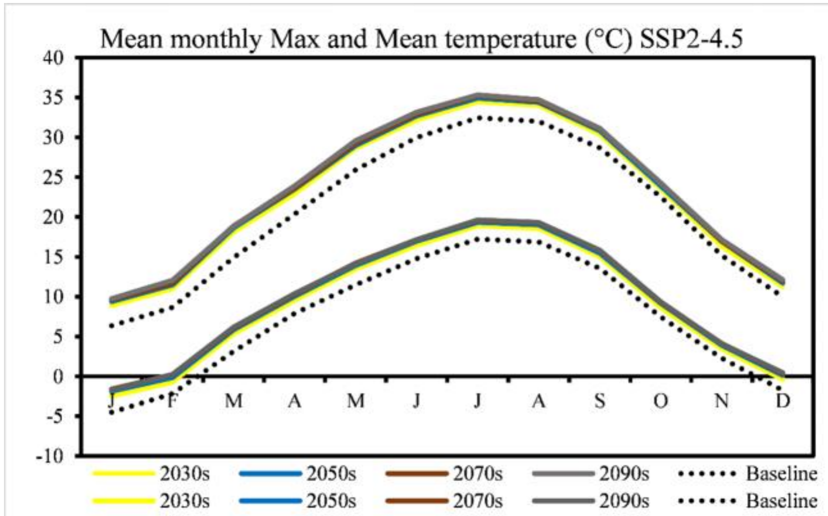

Figure 6. Projected ensemble-mean monthly maximum and minimum temperature under SSP2-4.5.

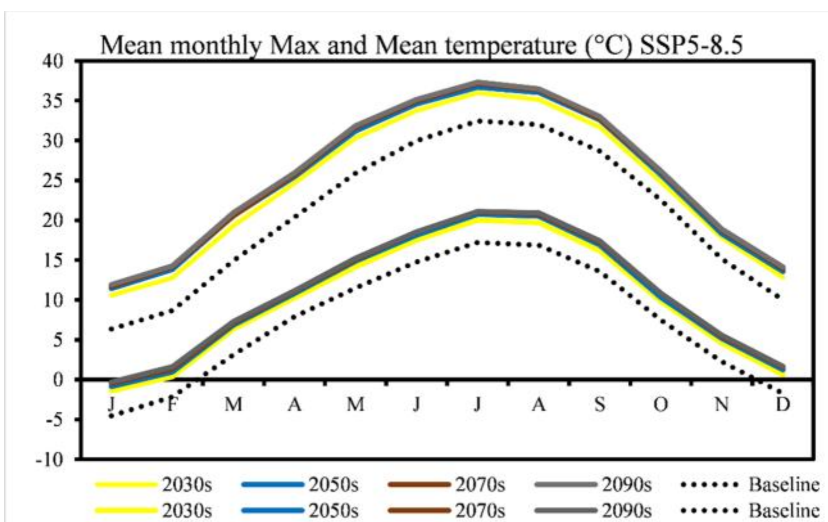

Figure 7. Projected ensemble-mean monthly maximum and minimum temperature under SSP5-8.5.

3.3. Precipitation projection

Precipitation in the study area compared to the baseline shows a change under SSP2-4.5 and SSP5-8.5 in the future. Figure 8 shows the mean seasonal and annual precipitation changes (%) for four mean ensembles of GCMs. The ensemble mean annual precipitation shows a decrease of 11.7%, 5.6%, 7.2%, and 7.8% under SSP2-4.5 for periods (the 2030s, 2050s, 2070s, and 2090s), and a decrease of 0.1% and 0.6% under SSP5-8.5 for the period 2030s and 2050s. On the contrary, for the 2070s and 2090s, projected annual precipitation increased by 5.4% and 4.7%, respectively.

On the seasonal level, precipitation increase steadily in the dry season (summer months) until the start of the wet season under both scenarios. However, the precipitation decreases from the wet season (winter to early spring) until the dry season (summer). Mean seasonal precipitation change by -23.7%, -17.9%, -17.9%, and -16.2% for the winter, -11.4%, -4.0%, -8.9%, and -10.6% for the spring, +30.3%, +50.3%, +55.7%, and +34.0% for the summer, +8.3%, +1.8%, +0.8%, and +8.7% for the autumn under SSP2-4.5. Similarly, change by -3.0%, -4.8%, -3.4% and -0.6% for the winter, -4.3%, -13.9%, +0.7%, and

-5.0% for the spring, +13.5%, +32.9%, +40.7%, and +31.5% for the summer, +19.5%, +42.4%, +36.3%, and +46.1% for the autumn under SSP5-8.5 compared to the baseline.

In spite of the projected decline in future precipitation under SSP2-4.5, the long-term mean monthly precipitation regime is not anticipated to drop during the year; different GCM show both positive and negative deviations from the baseline (Figure 9). The ensemble of selected GCMs shows a decrease of 23% to 17% in February under SSP2-4.5 and 3.6% to 30.8% in May under SSP5-8.5. There was a significant increase in precipitation in August, ranging from 68.4% to 94.6% under SSP2-4.5 and 49.9% to 70.2% in September under SSP5-8.5.The findings of this study are quite similar to UNEP 2016 results for Afghanistan, where future precipitation decreases under the optimistic scenario in CMIP5 till 2100, and spring precipitation decreases under the pessimistic scenario. Although the precipitation rate seems to increase in the dry season (Aich and A.J, 2016), precipitation declines during the wet season may significantly affect the area's water resources.

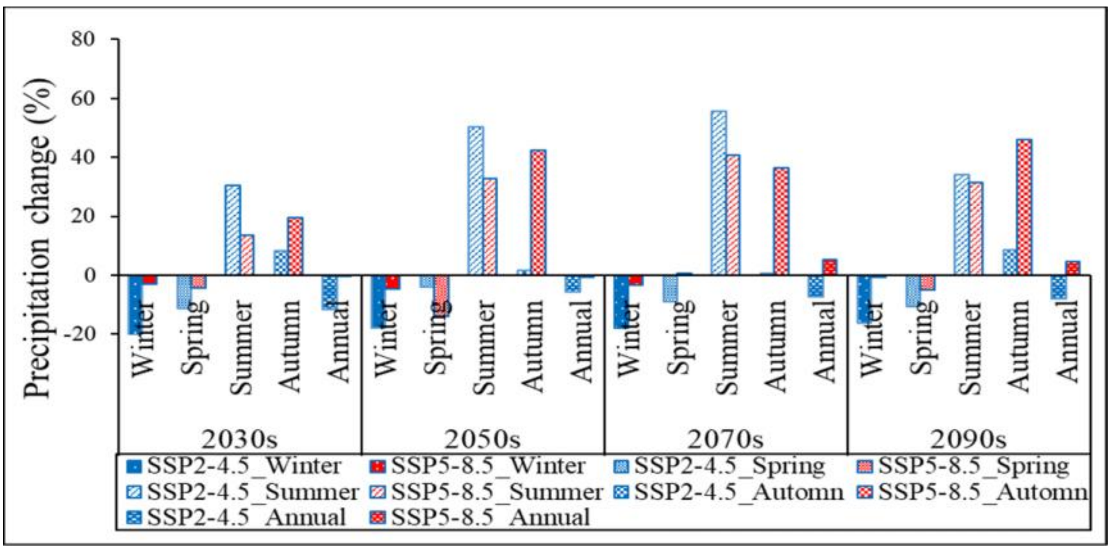

Figure 8. Projected ensemble-mean annual and seasonal precipitation relative change for the periods of 2022-2099 under the two SSP scenarios.

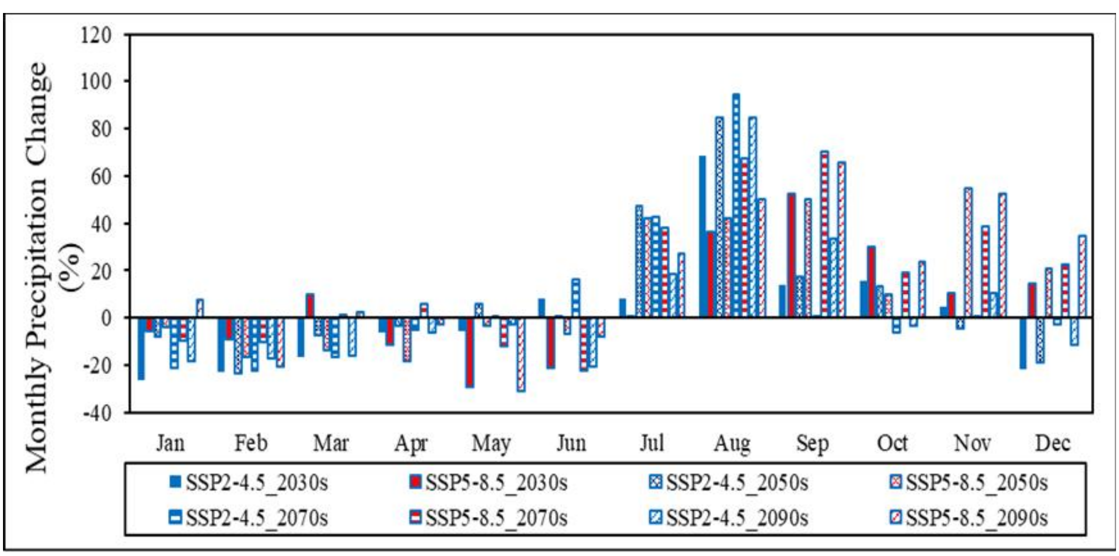

Figure 9. Projected ensemble-mean monthly precipitation relative changes for four time periods under SSP2-4.5 and SSP5-8.5.

3.4. SWAT calibration and validation

The SWAT model was calibrated and validated using 15 model parameters, as shown in Table 3. A comparison of SWAT-monthly simulated and observed monthly streamflow for the calibration (2006-2014) and validation periods (2015-2018) with precipitation is shown in Figure 10, and the scatter plots in Figure 11. During calibration and validation, the NSE values for the SWAT-simulated monthly streamflow versus the observation were 0.72 and 0.56, and the R^2 values were 0.72 and 0.60. The PBIAS values were 0.1% and 4.5%, and the RSR values were 0.53 and 0.66, respectively. Results were rated as "good" in calibration and "satisfactory" in the validation period.

The model effectively captures both low and high flow according to the depiction of the river discharge in Figure10 and the scatter plots in Fig. 11. In addition to the above, SWAT could not fully capture some of the high flows observed. With the concern of the existing conditions for simulation, which had a negative effect on the accuracy of the simulation, SWAT used the degree-day factor method to calculate snowmelt, which can't simulate snow with high accuracy (Raoof *et al.*, 2017). Also, the small area of the studied watershed and its low flow rate naturally cause the coefficient of variation in this data to be high, which decreases the simulation accuracy. Another issue that has played a negative role in the simulation is water consumption for agricultural use, with no reliable data available to apply to the model.

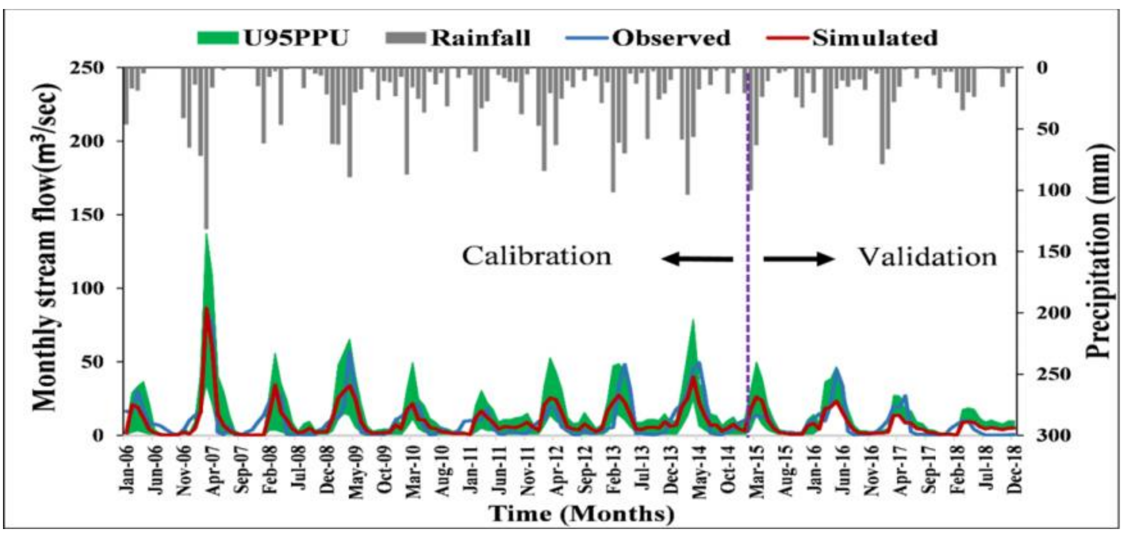

Fig. 10. SWAT simulated and observed monthly streamflow for calibration (2006-2014) and validation (2015-2018) periods.

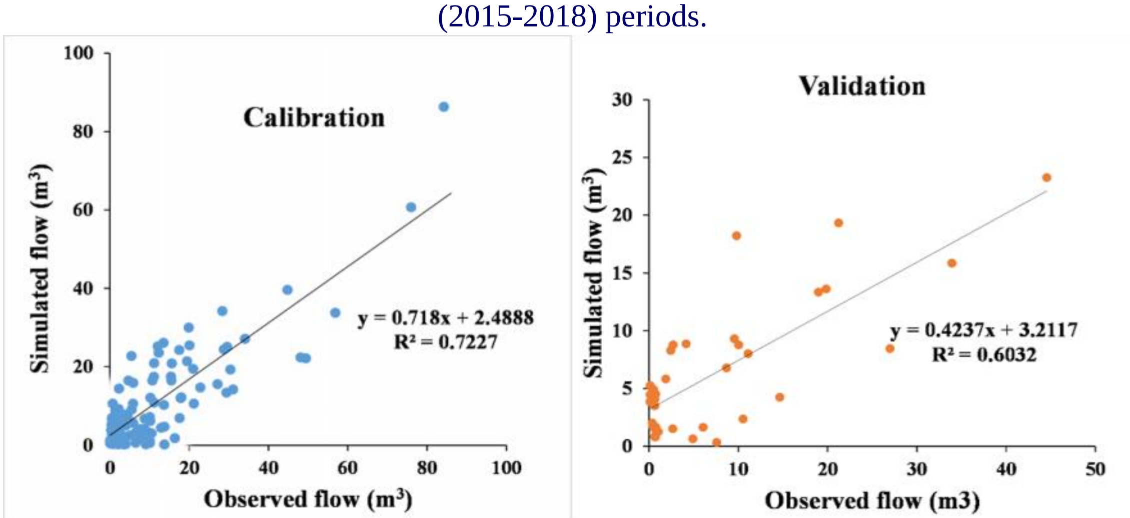

Fig. 11. scatter plots of observed and simulated streamflow for the calibration and validation period.

Table 3. parameters used for calibration and validation.

Rank	Parameters	Parameters description	Par.range MIN	Par.range MAX	Fitted values
1	v__PLAPS.sub	Precipitation lapse rate	0	100	0.494905
2	v__TLAPS.sub	Temperature lapse rate	-10	10	-3.346961
3	v__SFTMP.bsn	[OPTINAL] Snowfall temperature	-5	5	1.570583
4	v__SMTMP.bsn	Snow melt base temperature	-5	5	-1.660388
5	v__SMFMN.bsn	Minimum melt rate for snow	0	10	4.128043
6	v__SMFMX.bsn	Maximum melt factor (mm°C/day)	0	10	7.033943
7	v__GW_DELAY.gw	Groundwater delay (days)	0	500	15.235995
8	v__GWQMN.gw	Threshold depth of water in the shallow aquifer required for return flow to occur (mm)	0	5000	1.202260
9	v__GW_REVAP.gw	Groundwater "revap" coefficient	0.02	0.2	0.2
10	r__CN2.mgt	SCS curve Number	-0.3	0.3	-0.103984
11	v__CH_N2.rte	Manning's "n" value for the main channel	-0.01	0.3	0.2
12	v__ALPHA_BF.gw	Base flow alpha factor (days)	0	1	0.949094
13	v__TIMP.bsn	Snowpack temperature lag	0	1	0.9
14	r__SOL_AWC.sol	Available water capacity of the soil layer	0	1	0.203996
15	v__ESCO.bsn	Soil evaporation compensation factor	0	1	0.331219

Note: "v" means the parameter value which is replaced by the given value, and "r" represents the parameter value that is multiplied by (1 + a given value).

3.5. Projected changes in streamflow

Average monthly future simulated streamflow using two climate scenarios (SSP2-4.5 and SSP5-8.5) and an ensemble of four GCMs for the periods (the 2030s, 2050s, 2070s, and 2090s) were analyzed by comparing them with the baseline streamflow (2004-2020). We utilized the simulated streamflow for the baseline generated by LARS-WG produced baseline climate to reference future forecasts (Fig.12). Since models cannot generate the streamflow accurately as gauged on the ground for the base period, this method may assist in reducing the possible bias caused by synthetic meteorological data and also the hydrological model (Ma *et al.*, 2021). Figure 12 demonstrates that the projected baseline average monthly streamflow generated by the LARS-WG is typically similar to the measured streamflow. Three GCMs (MIROC6, MPI-ESM1-2-LR, and NESM3) projected that peak flow event times are expected to shift from April to March in the future. In addition, the mean monthly streamflow ensemble indicates the same shift of peak flow from April to March. The projected streamflow shows a decrease for all periods of SSP2-4.5 and the 2030s and 2050s of SSP5-8.5. In contrast, there is an increase in the 2070s and 2090s compared to the baseline period.

Annual streamflow shows the largest decreases by -12.0 under SSP2-4.5 and by -1.8% under SSP5-8.5, whereas it shows the highest increases by 5.1% in the 2070s in SSP5-8.5. On a seasonal basis, as shown in Fig.13 river discharge could fluctuate by -15.4%, -7.7%, -7.2%, -7.2% for the winter, -20.0%, -11.1%, -16.5%, -15.7% for spring, +4.2%, +15.9%, +17.2%, +6.3% for summer, and +8.3%, +19.0%, +19.9%, +24% for autumn under the SSP2-4.5 scenario. Similarly, river discharge under SSP5-8.5 could fluctuate by +2.18%, +5.4%, +6.4%, +9.29% for the winter, -7.9%, -21.4%, -6.4%, -9.1% for the spring, -7.1%, +8.1%, +11.0%, +8.8% for the summer, and +26.3%, +27.6%, +33.1%, +33.9% for the autumn season compared with the baseline period. On a monthly basis, under both SSPs scenarios, the ensemble-mean streamflow is projected to increase considerably in August by 19.3% to 52.2% under SSP52-4.5 and 30.0% to 68.3% under SSP5-8.5 for September. In the 2070s period under both SSPs, there is a larger increase in August streamflow than in the other three periods, as depicted in Fig. 14. Among the four GCMs, the median of NESM3 under both scenarios gave the highest annual decreasing streamflow trend, from 13.2% to 50.4%, and CanESM5 showed the highest streamflow increase trend, from 15.9% to 38.3%, under both SSPs, which correspond to the increased rainfall changes projected by these GCMs. The expected streamflow change is associated in future periods with the magnitude of rainfall and changes in temperature over the basin. The effect of expected changes in river discharge on water consumption planning can be significant. For instance, a decline in available river discharge during the winter season will put more strain on water supply, irrigation systems, and hydropower plants. In line with current findings, Zhai et al. (2020) concluded that in the northwest of South Asia including Afghanistan under CMIP6, the projections for the future 2020-2100 show an increase in water deficiency till the end of the 21st century due to a reduction in precipitation and a rise in temperature (Zhai et al., 2020). A decrease in water availability is mainly because of a reduction in precipitation and increased evapotranspiration due to temperature rise, and this illustrates the critical impact of global warming on the Kabul River basin's annual water availability (Bromand, 2015).

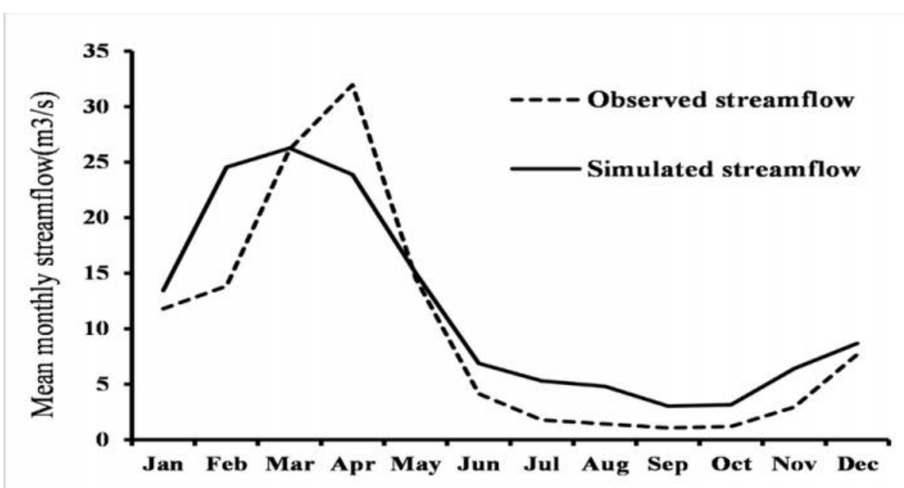

Figure 12. Observed mean monthly streamflow against streamflow driven by LARS-WG for the baseline.

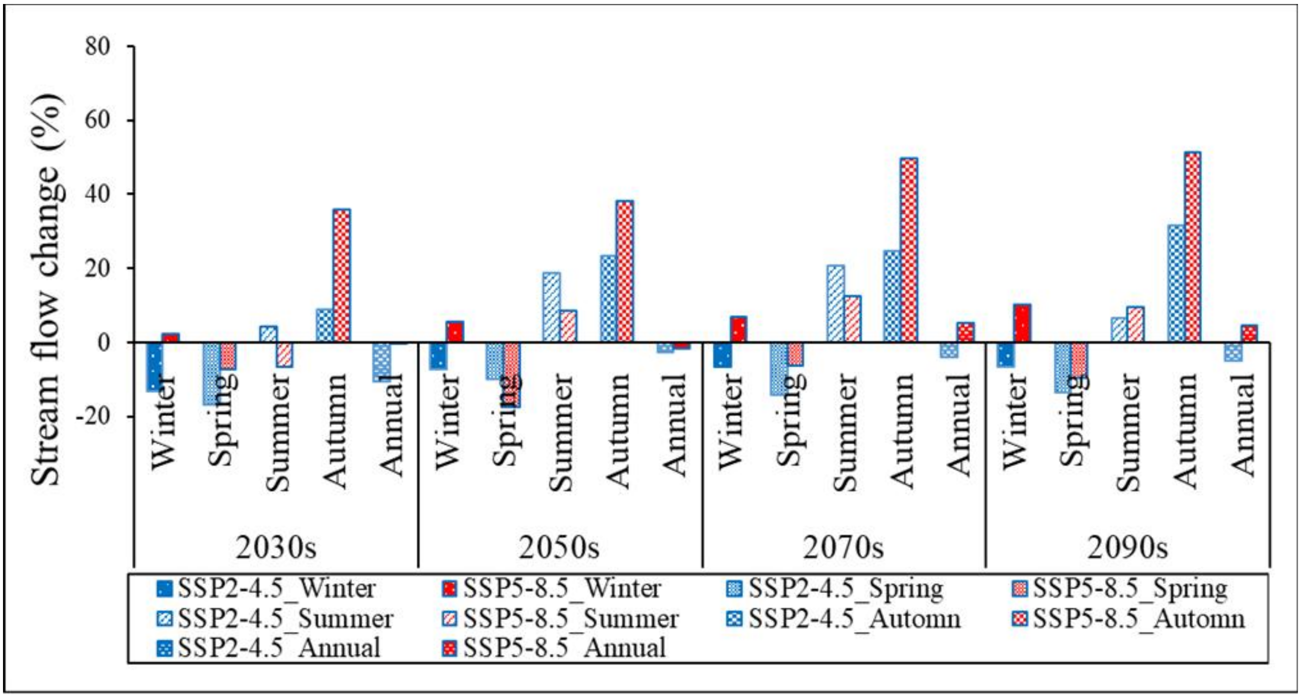

Figure 13. Projected ensemble-mean annual and seasonally relative changes in streamflow for the periods of 2022-2099 under the two SSP scenarios.

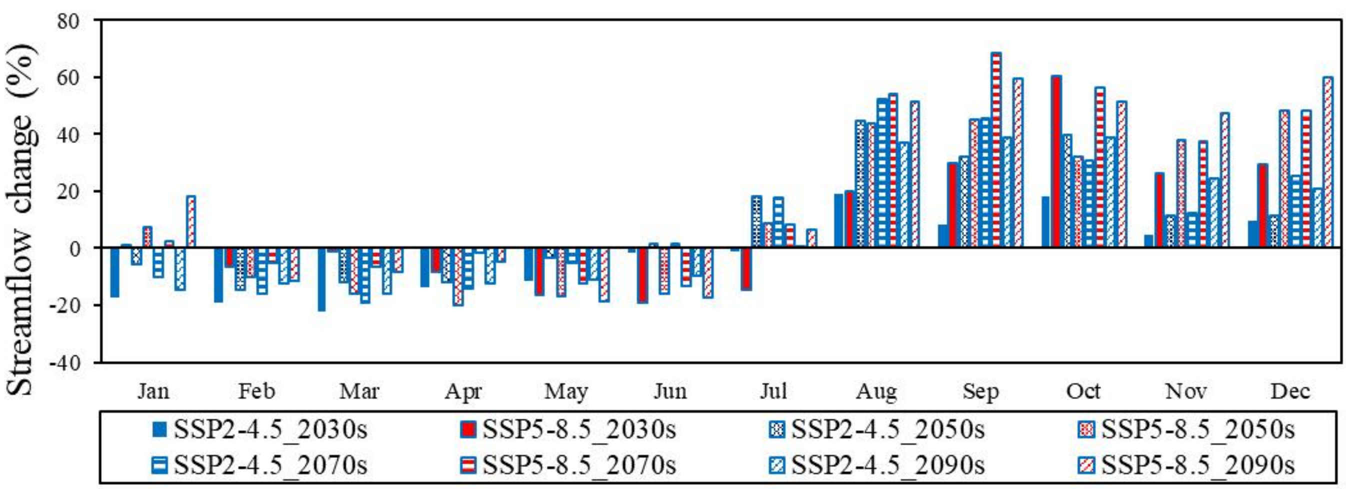

Figure14. Projected ensemble-mean monthly relative changes in streamflow for the periods of 2022-2099 under the two SSP scenarios.

4. Conclusion

An assessment of climate change's effects on water resources in the upper Kabul River Basin (KRB) was conducted in this study. Climate change was projected for four future periods (the 2030s, 2050s, 2070s, and 2090s) relative to the baseline (2004-2020) using an ensemble of four GCMs in CMIP6 under two emission scenarios (SSP2-4.5 and SSP5-8.5). For all four periods, every GCM projected an increase in the monthly mean maximum and minimum temperatures. The precipitation shows a decrease for the 21st century under SSP2-4.5 and for the periods 2030s and 2050s under SSP5-8.5, and an increase for the 2070s and 2090s under SSP5-8.5, decline is by -13.3% under SSP2-4.5 for2030s and a rise of 5.4% under SSP5-8.5 for 2070s.

The results showed a decrease in annual streamflow under SPP2-4.5 and SPP5-8.5, except for the 2070s and 2090s under SSP5-8.5, which shows a slight increase. Both scenarios showed a variation in mean-ensemble seasonal and annual streamflow from the present to the future due primarily to precipitation variability and increasing temperature. The seasonal impact would be more severe than the annual impact. Climate change could decrease streamflow during the wet season (winter to early spring) and increase flow during the dry season (summer). Increases in flow during the dry season are due to increased precipitation and increasing temperatures, which cause more snowmelt. According to the study, climate change will significantly impact water resources, and it observed inconsistent increases or decreases in water availability in the area. As a result, such research could assist hydro-climatologists and managers in making better scientific decisions about sustainable agriculture and sustainable water development in the face of climate change impacts.

Credit authorship contribution statement

Shahir Ahmad Taqizada: Investigation, Methodology, Formal analysis, Writing-original draft. **Xuejing Tang**: Formal analysis, Writing-review & editing. **Abdullah Ahmadi, Hellal Ahmad Taqizada:** Methodology, Formal analysis. **Zhenzhong Hu**: Validation, Conceptualization, Writing-review & editing Formal analysis.

Acknowledgments

This work was supported by Joint Funds of National Natural Science Foundation of China (U20A20302), Natural Science Foundation of Hebei Province (B2019202455), Overseas High-level Talents Introduction Plan Foundation of Hebei Province (E2019050012), Innovative Group Projects in Hebei Province (E2 021202006) and Fundamental Research Fundation of Hebei University of Technology (JBKYTD2001).

Conflict of Interest Statement

This manuscript has not been published and is not under consideration for publication elsewhere. We have no conflicts of interest to disclose.

References

Aawar, T., Khare, D., 2020. Assessment of climate change impacts on streamflow through hydrological model using SWAT model: a case study of Afghanistan. Modeling Earth Systems and Environment 6, 1427-1437.

Abbaspour, K.C., Vaghefi, S.A., Srinivasan, R., 2018. A guideline for successful calibration and uncertainty analysis for Soil and water assessment: a review of papers from the 2016 international SWAT conference. Water 10, 6.

Abbaspour, K.C., Yang, J., Maximov, I., Siber, R., Bogner, K., Mieleitner, J., Zobrist, J., Srinivasan, R., 2007. Modeling hydrology and water quality in the pre-alpine/alpine Thur watershed using SWAT. Journal of Hydrology 333, 413-430.

Aich, V., A.J, K., 2016. Afghanistan: Climate Change Science Perspectives. Kabul: National Environmental Protection Agency & UN Environment.

Alamdari, N., Sample, D.J., Steinberg, P., Ross, A.C., Easton, Z.M., 2017. Assessing the effects of climate change on water quantity and quality in an urban watershed using a calibrated stormwater model. Water 9, 464.

Alokozay, R., J, J., 2020. Impact of climate change on water resources in Kabul City. International Research Journal of Engineering and Technology (IRJET) 07, 1679.

Arnold, J.G., Srinivasan, R., Muttiah, R.S., Williams, J.R., 1998. Large area hydrologic modeling and assessment part I: model development. Journal of the American Water Resources Association. 34, 73-89.

Baghanam, A.H., Eslahi, M., Sheikhbabaei, A., Seifi, A.J., 2020. Assessing the impact of climate change over the northwest of Iran: an overview of statistical downscaling methods. Theoretical and Applied Climatology 141, 1135-1150.

Bromand, M.T., 2015. Impact assessment of climate change on water resources in the Kabul River Basin, Afghanistan. Master's thesis, Ritsumeikan University, Shiga, Japan.

Eyring, V., Bony, S., Meehl, G.A., Senior, C.A., Stevens, B., Stouffer, R.J., Taylor, K.E., 2016. Overview of the Coupled Model Intercomparison Project Phase 6 (CMIP6) experimental design and organization. Geoscientific Model Development 9, 1937-1958.

Ficklin, D.L., Luo, Y., Luedeling, E., Gatzke, S.E., Zhang, M., 2010. Sensitivity of agricultural runoff loads to rising levels of CO2 and climate change in the San Joaquin Valley watershed of California. Environmental Pollution 158, 223-234.

Galata, A., Tullu, K., Guder, A., 2020. Evaluating watershed hydrological responses to climate changes at Hangar Watershed, Ethiopia. Journal of Water and Climate Change.

Gassman, P.W., Sadeghi, A.M., Srinivasan, R., 2014. Applications of the SWAT model special section: overview and insights. Environmental Quality 43, 1-8.

Ghulami, M., 2017. Assessment of climate change impacts on water resources and agriculture in data-scarce Kabul basin, Afghanistan. Ph.D. Dissertation, Université Côte d'Azur.

Golladay, S.W., Craig, L.S., DePalma-Dow, A.D., Emanuel, B.N., Rogers, S.G., 2020. Building resilience into water management through public engagement. Freshwater Science 40, 238-244

Gusain, A., Ghosh, S., Karmakar, S., 2020. Added value of CMIP6 over CMIP5 models in simulating Indian summer monsoon rainfall. Atmospheric Research 232, 104680.

Hashmi, M.Z.U.R., Masood, A., Mushtaq, H., Bukhari, S.A.A., Ahmad, B., Tahir, A.A., 2020. Exploring climate change impacts during first half of the 21st century on flow regime of the transboundary Kabul River in the Hindukush region. Journal of Water and Climate Change 11, 1521-1538.

Hyandye, C.B., Worqul, A., Martz, L.W., Muzuka, A.N.N., 2018. The impact of future climate and land use/cover change on water resources in the Ndembera watershed and their mitigation and adaptation strategies. Environmental Systems Research 7, 7.

Khalid, K., Ali, M.F., Abd Rahman, N.F., Mispan, M.R., Haron, S.H., Othman, Z., Bachok, M.F., 2016. Sensitivity analysis in watershed model using SUFI-2 algorithm. Procedia Engineering 162, 441-447.

Khoi, D.N., Nguyen, V., Sam, T. T. Nhi, P. T. T, 2019. Evaluation on effects of climate and land-use changes on streamflow and water quality in the La Buong River Basin, Southern Vietnam. Sustainability 11, 7221

Khoi, D.N., Sam, T. T., Nhi, P. T. T., Quan, N. T., Hung, B. V., Phung, N. K. Van Thinh, N. , 2019. Uncertainty assessment for climate change impact on streamflow and water quality in the dong nai river basin, Vietnam. World Environmental and Water Resources Congress 2019. American Society of Civil Engineers Reston, VA, 366-373.

King, L.M., Irwin, S., Sarwar, R., McLeod, A.I.A., Simonovic, S.P., 2012. The effects of climate change on extreme precipitation events in the Upper Thames River Basin: a comparison of downscaling approaches. Canadian Water Resources Journal 37, 253-274.

Kurylyk, B.L., MacQuarrie, K.T., McKenzie, J.M., 2014. Climate change impacts on groundwater and soil temperatures in cold and temperate regions: Implications, mathematical theory, and emerging simulation tools. Earth-Science Reviews 138, 313-334.

Lashkaripour, G.R., Hussaini, S.A., 2008. Water resource management in Kabul river basin, eastern Afghanistan. Environmentalist 28, 253-260.

Ma, D., Qian, B., Gu, H., Sun, Z., Xu, Y.P., 2021. Assessing climate change impacts on streamflow and sediment load in the upstream of the Mekong River basin. International Journal of Climatology 41, 3391-3410.

Mateo-García, G., Gómez-Chova, L., Amorós-López, J., Muñoz-Marí, J., Camps-Valls, G., 2018. Multitemporal cloud masking in the Google Earth Engine. Remote sensing 10, 1079.

Moriasi, D.N., Arnold, J.G., Van Liew, M.W., Bingner, R.L., Harmel, R.D., Veith, T.L., 2007. Model evaluation guidelines for systematic quantification of accuracy in watershed simulations. American Society of Agricultural and Biological Engineers 50, 885-900.

Nafees, M., Shabir, A., Zahid, U., 2016. Construction of dam on Kabul River and its socio-economic implication for Khyber Pukhtunkhwa, Pakistan. Seminar on "Pak–Afghan Water Sharing Issue 23, 2016.

Nasimi, M.N., Sagin, J., Wijesekera, N., 2020. Climate and water resources variation in Afghanistan and the need for urgent adaptation measures. International Journal of Food Science and Agriculture 4, 49-64.

Neitsch, S.L., Arnold, J.G., Kiniry, J.R., Williams, J.R., 2011. Soil and water assessment tool theoretical documentation version 2009. Texas Water Resources Institute.

Nyatuame, M., Amekudzi, L.K., Agodzo, S.K., 2020. Assessing the land use/land cover and climate change impact on water balance on Tordzie watershed. Remote Sensing Applications: Society and Environment 20, 100381.

O'Neill, B.C., Tebaldi, C., van Vuuren, D.P., Eyring, V., Friedlingstein, P., Hurtt, G., Knutti, R., Kriegler, E., Lamarque, J.-F., Lowe, J., 2016. The scenario model intercomparison project (ScenarioMIP) for CMIP6. Geoscientific Model Development 9, 3461-3482.

Phan, T.N., Kuch, V., Lehnert, L.W., 2020. Land cover classification using Google Earth Engine and random forest classifier—The role of image composition. Remote sensing 12, 2411.

Ramirez-Villegas, J., Challinor, A.J., Thornton, P.K., Jarvis, A., 2013. Implications of regional improvement in global climate models for agricultural impact research. Environmental Research Letters 8, 024018.

Raoof, M., Azizi, M., Salahshour, A., 2017. Estimating hydrological and hydrogeological parameters of watershed using SWAT model (Case study: Balukhlu-chay Basin). Water and Soil Science 26, 173-185.

Rasouli, H., Kayastha, R.B., Bhattarai, B.C., Shrestha, A., Arian, H., Armstrong, R., 2015. Estimation of discharge from Upper Kabul River Basin, Afghanistan using the snowmelt runoff model. Journal of Hydrology and Meteorology 9, 85-94.

Riahi, K., van Vuuren, D.P., Kriegler, E., Edmonds, J., O'neill, B.C., Fujimori, S., Bauer, N., Calvin, K., Dellink, R., Fricko, O., 2017. The shared socio-economic pathways and their energy, land use, and greenhouse gas emissions implications: an overview. Global Environmental Change 42, 153-168.

Sao, D., Kato, T., Tu, L.H., Thouk, P., Fitriyah, A., Oeurng, C., 2020. Evaluation of different objective functions used in the SUFI-2 calibration process of SWAT-CUP on water balance analysis: A Case Study of the Pursat River Basin, Cambodia. Water 12, 2901.

Shrestha, B., Babel, M., Maskey, S., Griensven, A.v., Uhlenbrook, S., Green, A., Akkharath, I., 2013. Impact of climate change on sediment yield in the Mekong River basin: a case study of the Nam Ou basin, Lao PDR. Hydrology and Earth System Sciences 17, 1-20.

Sidiqi, M., Shrestha, S., Ninsawat, S., 2018. Projection of climate change scenarios in the Kabul River Basin, Afghanistan. Current Science 114, 1304-1310.

Skoulikaris, C., Anagnostopoulou, C., Lazoglou, G., 2020. Hydrological modeling response to climate model spatial analysis of a South Eastern Europe International Basin. Climate 8, 1.

Tan, M.L., Gassman, P., Yang, X., Haywood, J., 2020. A review of SWAT applications, performance and future needs for simulation of hydro-climatic extremes. Advances in Water Resources 143, 103662.

Tan, M.L., Gassman, P.W., Srinivasan, R., Arnold, J.G., Yang, X., 2019. A review of SWAT studies in Southeast Asia: applications, challenges and future directions. Water 11, 914.

Teutschbein, C., Seibert, J., 2012. Bias correction of regional climate model simulations for hydrological climate-change impact studies: Review and evaluation of different methods. Journal of Hydrology 456, 12-29.

The CMIP6 landscape, 2019. Nature Climate Change 9, 727.

Touma, D., Ashfaq, M., Nayak, M.A., Kao, S.-C., Diffenbaugh, N.S., 2015. A multi-model and multi-index evaluation of drought characteristics in the 21st century. Journal of Hydrology 526, 196-207.

Wang, H., Stephenson, S.R., 2018. Quantifying the impacts of climate change and land use/cover change on runoff in the lower Connecticut River Basin. Hydrological process 32, 1301-1312.

Wang, J., Hu, L., Li, D., Ren, M., 2020. Potential impacts of projected climate change under CMIP5 RCP scenarios on streamflow in the Wabash River Basin. Advances in Meteorology 2020, 18.

Wi, S., Yang, Y., Steinschneider, S., Khalil, A., Brown, C., 2015. Calibration approaches for distributed hydrologic models in poorly gauged basins. Hydrology and Earth System Sciences. 19, 857–876.

Willems. P, Vrac. M, 2011. Statistical precipitation downscaling for small-scale hydrological impact investigations of climate change. Journal of Hydrology 402, 193-205.

Yu, Z., Man, X., Duan, L., Cai, T., 2020. Assessments of impacts of climate and forest change on water resources using SWAT model in a sub-boreal watershed in Northern Da Hinggan Mountains. Water 12, 1565.

Zaryab, A., Noori, A.R., Wegerich, K., Kløve, B., 2017. Assessment of water quality and quantity trends in Kabul Aquifers with an outline for future water supplies. Central Asian Journal of Water Research 3, 1925.

Zhai, J.Q., Mondal, S.K., Fisher, T., Wang, Y.J., Su, B.D ., Huang, J.L., Tao, H., Wang, G.J., Ullah, W., Uddin, M.J, 2020. Future drought characteristics through a multi-model ensemble from CMIP6 over South Asia. Atmospheric Research 246, 105111.

Zhang, S., Li, Z., Lin, X., Zhang, C., 2019. Assessment of climate change and associated vegetation cover change on watershed-scale runoff and sediment yield. Water 11, 1373.

Access this Article in Online	
	Website: www.ijarm.com
Quick Response Code	Subject: Hydrology
DOI:10.22192/ijamr.2022.09.08.005	

How to cite this article:
Shahir Ahmad Taqizada, Xuejing Tang, Abdullah Ahmadi, Hellal Ahmad Taqizada, Zhenzhong Hu. (2022). Impact of climate change on hydrology based on multi-model ensemble of CMIP6 in the Upper Kabul River Basin, Afghanistan. Int. J. Adv. Multidiscip. Res. 9(8): 35-56.
DOI: http://dx.doi.org/10.22192/ijamr.2022.09.08.005